Synthesis and dielectric properties of polyaniline/titanium dioxide nanocomposites

Te-Cheng Mo [a], Hong-Wen Wang [b,*], San-Yan Chen [a], Yun-Chieh Yeh [b]

[a] *Department of Materials Science and Engineering, National Chiao-Tung University, Hsinchu 30049, Taiwan, ROC*
[b] *Department of Chemistry, Chung-Yuan Christian University, Chungli 32023, Taiwan, ROC*

Abstract

Two series of polyaniline–TiO_2 nanocomposite materials were prepared in base form by in situ polymerization of aniline with inorganic fillers using TiO_2 nanoparticles (P25) and TiO_2 colloids (Hombikat), respectively. The effect of particle sizes and contents of TiO_2 materials on their dielectric properties was evaluated. The as-synthesized polyaniline–TiO_2 nanocomposite materials were characterized by transmission electron microscopy (TEM), Fourier transform infrared (FTIR), thermal analysis (DTA/TGA), and X-ray diffraction (XRD). Dielectric properties of polyaniline–TiO_2 nanocomposites in the form of films were measured at 1 KHz–1 MHz and a temperature range of 35–150 °C. Higher dielectric constants and dielectric losses of polyaniline–TiO_2 nanocomposites than those of neat PANI were found. PANI–TiO_2 nanocomposites derived from P25 exhibited higher dielectric constants and losses than those from Hombikat TiO_2 colloids. Electrical conductivity measurements indicate that the conductivity of nanocomposites is increased with TiO_2 content. The dielectric properties and conductivities are considered to be enhanced due to the addition of TiO_2, which might induce the formation of a more efficient network for charge transport in the base polyaniline matrix.
© 2007 Elsevier Ltd and Techna Group S.r.l. All rights reserved.

Keywords: B. Nanocomposite; C. Dielectric properties; Polyaniline/TiO_2

1. Introduction

The creation of polymer/inorganic nanoparticle composites having unique physical properties has attracted intensive research recently [1–8]. Polymeric materials with high-dielectric constants are highly desirable for use in actuators, artificial muscles, and charge-storage devices [1,2]. To raise the dielectric constant of polymers, high-dielectric constant ceramic powders such as $BaTiO_2$ and $PbTiO_3$ were added to the polymers to form nanocomposites [3–8]. Polyaniline (PANI) is the most attractive conducting polymer due to its low cost, high environmental stability, good electrical conductivity and potential applications in molecular electronics. The electrical properties of polyaniline could be modified by the addition of inorganic fillers [18–23]. Nanoscale fillers are the most attractive, due to intriguing properties arising from the nanosize and large surface area. The insertion of nanoscale

fillers may improve the electrical and dielectric properties of host polyaniline materials. A very high-dielectric constant – up to 3700 for polyaniline–TiO_2 nanocomposite materials – was reported by Dey et al. [22]. However, high-dielectric constants are usually accompanied with high-dielectric losses [9–17,23]. Xu et al. [24] noticed that the electrical conductivity of a PANI–TiO_2 nanocomposite with a low TiO_2 content is much higher than of neat PANI. Su et al. [25] reported that the PANI–TiO_2 nanocomposite has suitable conductivity (1–10 S/cm), and increases after thermal treatment at 80 °C for 1 h. The reason for the ultrahigh dielectric properties of PANI–TiO_2 nanocomposites is not clear [22]. In the present study, TiO_2 with two different particle sizes is employed to modify base form polyaniline. The dielectric properties of polyaniline–TiO_2 nanocomposites were characterized. Enhanced, but not ultrahigh, dielectric constants were observed.

2. Experimental procedure

Aniline (99%, Fluka) was doubly distilled under a reduced pressure. Both 1.0 M NH_4OH and 1.0 M HCl were prepared by

* Corresponding author. Tel.: +886 3 2653310; fax: +886 3 2653399.
E-mail address: hongwen@cycu.edu.tw (H.-W. Wang).

diluting concentrated ammonia and hydrochloric acid with de-ionized water for the acidic and basic aqueous media, respectively. 1-Methy-2-pyrrolidinone (NMP) (99.7%, Mallinckrodt) was used as received without further purification. Ammonium persulfate (Showa, 98%) was employed as oxidant. Two types of TiO_2 were employed. P-25, average particle size 50 nm, was purchased from Showa Tokyo Japan. Hombikat TiO_2 colloids, average particle size 25 nm, were purchased from Sachtleben Chemie Germany.

An appropriate amount of organophilic TiO_2 (1–5 wt% to that of polyaniline) was introduced into 400 ml of 1.0 M HCl while magnetically stirring overnight at room temperature. An aniline monomer (0.1 mol) was subsequently added to the solution and stirred for 24 h. Upon addition of ammonium persulfate (0.025 mol) into 20 ml of 1.0 M HCl, the solution was stirred for 3 h at 5 °C in an ice bath. The as-synthesized HCl-doped lamellar nanocomposites precipitates were obtained by filtering and drying under a dynamic vacuum at room temperature for 48 h. The final products were bathed using 400 ml of 10.0 M NH_4OH at room temperature while magnetically stirring for 4 h, followed by filtration and drying under vacuum for 48 h.

Characterization of the structures of as-synthesized nanocomposites was accomplished using wide-angle powder X-ray diffraction (WAXRD) in order to examine the TiO_2 phase. Transmission electron microscopy (TEM) was employed to image the TiO_2 dispersion in the polyaniline matrix. The WAXRD studies were performed on a Rigaku D/MAX-3C X-ray diffractometer with a Cu target and Ni filter at a scanning rate of 4°/min. The sample for the TEM study was prepared by hardening polyaniline–TiO_2 nanocomposites thin films into an epoxy resin at 80 °C for 24 h in a vacuum oven. Then, the cured epoxy resin containing nanocomposites was microtomed into 60–90 nm slices with a Reichert-June Ultracut-E. Subsequently, one layer of carbon about 10 nm thick was deposited on the slices on mesh 300 copper nets for TEM observations on a JEOL-200FX with an acceleration voltage of 120 kV. Fourier transform infrared (FTIR) spectra were obtained at a resolution of 4.0 cm^{-1} with an FTIR (BIO-RAD FTS-7) at room temperature ranging from 4000 to 400 cm^{-1}. The FTIR spectra provided further evidences that TiO_2 was dispersed within the polyaniline matrix.

A vacuum evaporated gold electrode was deposited on both sides of the nanocomposite film (electrode area 0.5625 cm^2) after drying at 80 °C overnight before the dielectric characterization. ac resistance and dielectric parameters such as the capacitance and dissipation factor (tan δ) were measured by a Agilent 4284 LCR precision meter at various frequencies (1 KHz–1 MHz) under temperatures from 30–100 °C. The thickness of the sample was 60–80 μm. The dielectric constants (ε_r) of the specimens were calculated by the equation:

$$C = \varepsilon_r \varepsilon_0 \frac{A}{d}$$

where ε_0 is the vacuum permittivity, which equals 8.85×10^{-12} F/m; "A" is the electrode area; and "d" is the thickness of the specimen. The ac conductivities, σ, of the
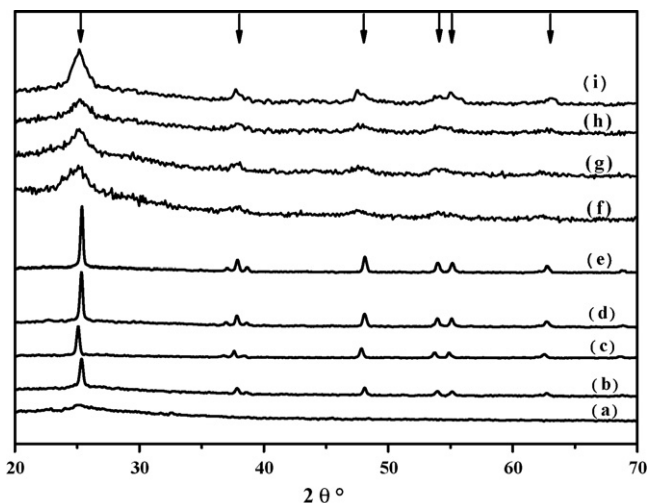

Fig. 1. The XRD diffraction patterns for polyaniline–TiO_2 nanocomposites obtained from (a) pure PANI, (b) PANI with 1 wt% TiO_2-P25, (c) PANI with 3 wt% TiO_2-P25, (d) PANI with 5 wt% TiO_2-P25, (e) pure TiO_2-P25, (f) PANI with 1 wt% TiO_2-Hombikat, (g) PANI with 3 wt% TiO_2-Hombikat, (h) PANI with 5 wt% TiO_2-Hombikat, and (i) pure TiO_2-Hombikat. The arrows indicated the peaks of the anatase phase.

specimens were calculated from the measured resistance by the LCR meter at a frequency of 1 kHz–1 MHz.

3. Results and discussion

3.1. XRD and FTIR

Fig. 1 shows the WAXRD diffraction patterns for a series of pure polyaniline and PANI–TiO_2 nanocomposite materials. The anatase TiO_2 had 2θ values at 25.27°, 37.78°, 48.07°, 53.92°, 55.11°, 62.72°. Fig. 1(a) shows that a small peak is around $2\theta = 25$°, indicating the PAIN also exhibits some degree of crystallinity. For PANI–TiO_2 (P25) nanocomposites, peaks of the TiO_2 anatase phase are clear, as shown in Fig. 1(b)–(d). Comparing curves (b)–(d) with (e), it is clear that diffraction
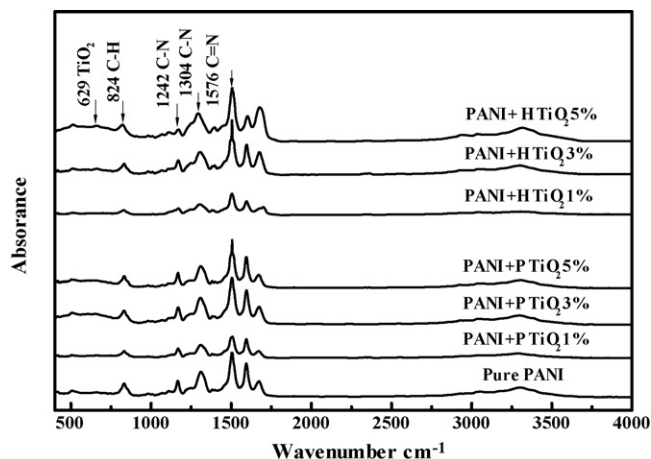

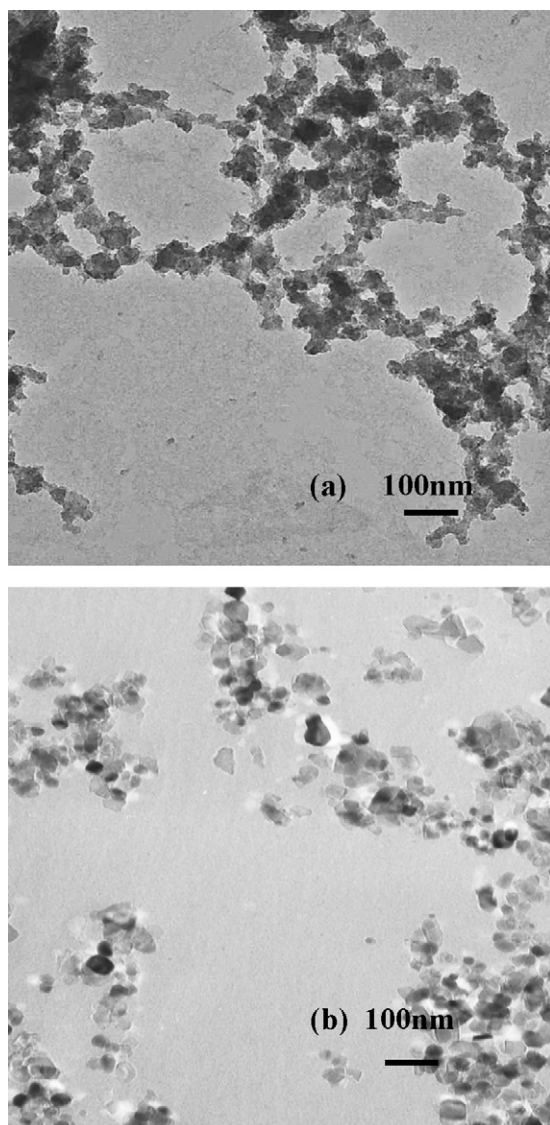Fig. 2. FTIR curves for PANI and polyaniline–TiO_2 nanocomposites. P: P25, H: Hombikat.

Fig. 3. TEM for PANI–TiO$_2$ nancomposites (a) PANI with 3 wt% TiO$_2$-Hombikat and (b) PANI with 3 wt% TiO$_2$-P25.
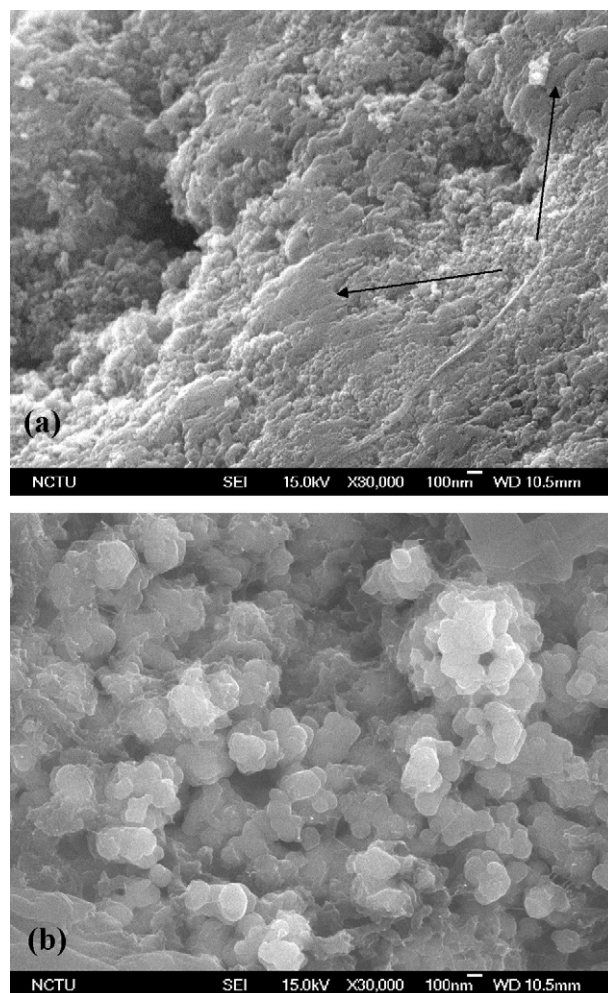

Fig. 4. SEM for polyaniline–TiO$_2$ nancomposites. (a) PANI with 5 wt% TiO$_2$-Hombikat, some flat large lumps are observed (arrow indicates); (b) PANI with 5 wt% TiO$_2$-P25.

patterns of the polyaniline–TiO$_2$ composites are identical to those of TiO$_2$ P25 particles. This implies that polyaniline deposited on the surface of nano-TiO$_2$ particles has no effect on the crystallization performance of P25 nanoparticles. However, for the PANI–TiO$_2$ (Hombikat) nanocomposites, very broad peaks are exhibited (curve (f)–(h)), which implies the poor crystallinity nature of Hombikat TiO$_2$ colloids.

Fig. 2 shows the FTIR spectra for pure polyaniline and the PANI–TiO$_2$ nanocomposite materials. The main characteristic peaks are assigned as follows: the band at 1576 cm^{-1} is attributed to C=N stretching mode, 1242 and 1304 cm^{-1} have been attributed to the C–N stretching mode for the quinonoid and benzenoid units. The peak at 824 cm^{-1} is associated with C–C and C–H for a benzenoid unit. Both PANI–TiO$_2$ nanocomposites show very similar spectra to that of pristine PANI. TiO$_2$ peaks at 629 cm^{-1} are very weak in the studied nanocomposites. This result was similar to those of Yang's report [26].

3.2. TEM and SEM

Fig. 3(a) and (b) show the TEM images for the PANI-3% TiO$_2$-hombikat and the PANI-3% TiO$_2$ P25, respectively. As shown in Fig. 3(a), particles of TiO$_2$-hombikat, having a crystal size of about 25 nm, tend to be agglomerated. In Fig. 3(b), particles of P25, having crystal sizes of 50 nm, are more discretely distributed. SEM micrographs for the crack surface of PANI–TiO$_2$ nanocomposites are showed in Fig. 4(a) and (b). In Fig. 4(a), the small and uniform spheres of Hombikat TiO$_2$ are observed. However, some flat large lumps within the PANI matrix are also identified (arrow indicates). In Fig. 4 (b), the particles of P25 are clear and covered by PANI materials. The distribution and packing of P25 in the PANI matrix is more uniform, and no large lumps are observed.

3.3. Dielectric properties and conductivity

To illustrate the effect of TiO$_2$ on the electrical properties of PANI materials, a comparison of PANI and PANI–TiO$_2$ nanocomposites was made. Figs. 5 and 6 show the dielectric
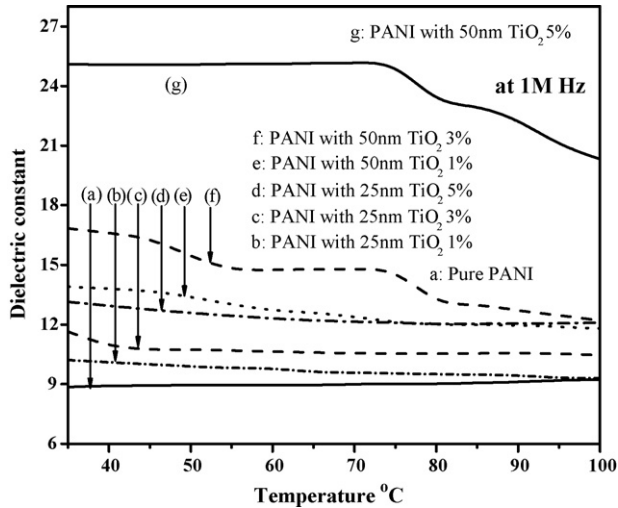
Fig. 5. Dielectric constant of PANI–TiO$_2$ nanocomposites at various temperatures. (a) Pure PANI, (b) PANI-1 wt% Hombikat, (c) PANI-3 wt% Hombikat, (d) PANI-5 wt% Hombikat, (e) PANI-1 wt% P25, (f) PANI-3 wt% P25 (g) PANI-1 wt% P25.

Fig. 7. Dielectric constant of PANI–TiO$_2$ nanocomposites at various frequencies. (a) Pure PANI, (b) PANI-1 wt% TiO$_2$ Hombikat, (c) PANI-3 wt% TiO$_2$ Hombikat, (d) PANI-5 wt% TiO$_2$ Hombikat, (e) PANI-1 wt% P25, (f) PANI-3 wt% P25, (g) PANI-5 wt% P25.

constants and dielectric losses of polyaniline at various TiO$_2$ contents from room temperature to 100 °C. As the content of TiO$_2$ increased, the dielectric constant and loss also increased. P25, with a particle size of about 50 nm, exhibits higher dielectric constants and losses than those of Hombikat TiO$_2$ colloids. The pristine PANI film in base form has a dielectric constant around 8.9 at 1 MHz, as shown in Fig. 5. P25 enhances the dielectric constant up to 25.5 at 5 wt% content under 1 MHz. However, high-dielectric constants accompanied with higher dielectric losses were observed in this study. From Figs. 5 and 6, 50 nm P25 TiO$_2$ enhances dielectric constants and losses, while 25 nm Hombikat TiO$_2$ colloids appear insignificant. Fig. 7 illustrates the diagram for dielectric constants versus frequencies for all PANI–TiO$_2$ nanocomposites. It was observed that 5 wt% P25 enhanced the dielectric constant of the PANI–TiO$_2$ nanocomposite up to 146 at 1 kHz, which is about 8
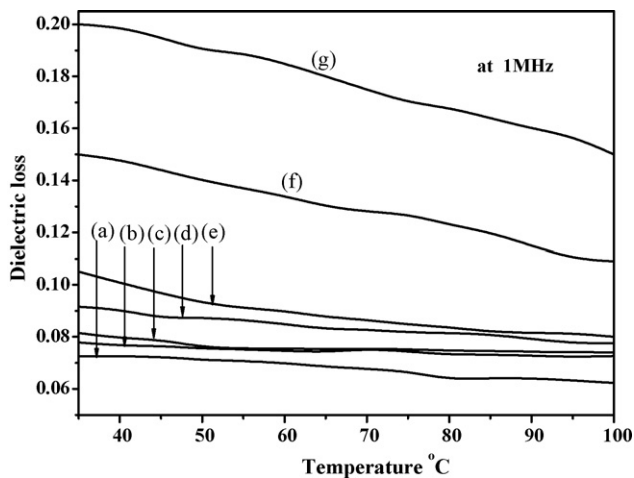
times that of pristine PANI under the same conditions. In the mean time, the dielectric loss for PANI-5% TiO$_2$ (P25) is also high ($\sim$0.8 at 1 kHz at room temperature), 10 times of pristine PANI at the same condition.

Fig. 8 shows the effect of P25 and Hombikat TiO$_2$ materials on the AC conductivity of PANI under 1 kHz, 10 kHz, and 1 MHz. Curves a–c are for 25 nm TiO$_2$-Hombikat and curves d–f are for 50 nm P25. In general, the conductivity of PANI-P25 is higher than those of PANI-Hombikat. Moreover, the conductivity of nanocomposites increases as the addition of TiO$_2$ increases from 1 to 5 wt%. The increasing tendency of conductivity for PANI–TiO$_2$ was also reported by Xu [24] and Su [25]. From the results described above, it has been considered that the enhanced dielectric constants and losses might originate from the increased conductivity. The addition of TiO$_2$ might induce the formation of a more efficient network

Fig. 6. Dielectric loss of PANI-TiO$_2$ nanocomposites at various temperatures. (a) Pure PANI, (b) PANI-1 wt% Hombikat, (c) PANI-3 wt% Hombikat, (d) PANI-5 wt% Hombikat, (e) PANI-1 wt% P25, (f) PANI-3 wt% P25, (g) PANI-1 wt% P25.
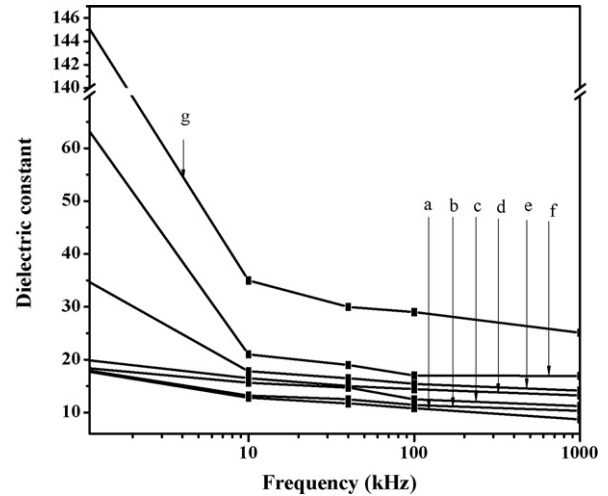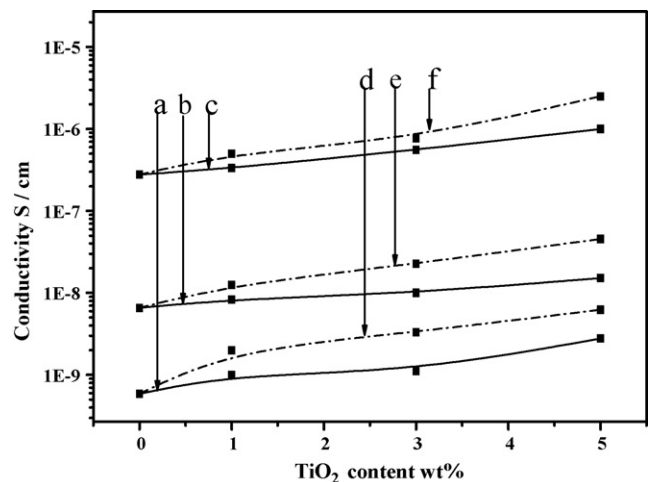

Fig. 8. ac conductivities of PANI–TiO$_2$ nanocomposites at 35 °C. (a) Hombikat 1 KHz, (b) Hombikat 10 KHz, (c) Hombikat 1 MHz, (d) P25 1 KHz, (e) P25 10 KHz, (f) P25 1 MHz.

for charge transport in the base polyaniline matrix, resulting in higher conductivities [24,27]. As shown in TEM and SEM micrographs, the distribution of 50 nm TiO_2 particles (P25) is more uniform than that of 25 nm TiO_2 powders. The uniformity of particle distribution in the case of P25 may result in a better network for charge transport than the non-uniform case (Hombikat).

4. Conclusion

A series of polyaniline–TiO_2 nanocomposite materials were prepared using an in situ polymerization process. From the characterization of SEM, TEM and X-ray diffraction, it was identified that the fine TiO_2 colloids (Hombikat) form a relatively non-uniform distribution in the PANI matrix, while P25 is more uniformly distributed. Dielectric characterization demonstrated that TiO_2 nanoparticles exhibit a strong effect on the dielectric properties of resultant PANI–TiO_2 nanocomposites. The uniform packing of P25 TiO_2 results an enhanced conductivity of the base form of the polyaniline film and thus enhances dielectric constants and losses. The increased conductivity is attributed to the formation of a better charge transport network in the relatively insulating polyaniline matrix.

References

[1] H.S. Nalwa, Handbook of Low and High Dielectric Constant Materials and Their Applications, Academic, San Diego, CA, 1999.

[2] B.C. Yoseph, Electroactive Polymer (EAP) Actuators as Artificial Muscles: Reality, Potential and Challenges, SPIE, WA, 2004.

[3] H. Banno, K. Ogura, Theoretical equations for dielectric, piezoelectric and elastic properties of flexible composite consisting of polymer and ceramic powder of two different materials, Ferroelectrics 95 (1989) 111–115.

[4] X.X. Huang, Z.F. Chen, W.Q. Zou, Y.S. Liu, J.D. Li, Long-term polarization relaxation effects in semicrystalline PVDF films, Ferroelectrics 101 (1990) 111–119.

[5] J.B. Ngoma, J.Y. Cavaille, J. Paletto, J. Perez, F. Macchi, Dielectric and piezoelectric properties of copolymer–ferroelectric composite, Ferroelectrics 109 (1990) 205–210.

[6] K.D. Dilip, Pyroelectricity in polymer, Ferroelectrics 118 (1991) 165–189.

[7] B. Wei, Y. Daben, Dielectric and piezoelectric properties of 0–3 composite film in PCM/PVDF and PZT/PVDF, Ferroelectrics 157 (1–4) (1994) 427–430.

[8] H.L.W. Chan, M.C. Cheung, C.L. Choy, Study on BaTiO3P(VDF-TrFE) 0–3 composites, Ferroelectrics 224 (1–4) (1999) 113–120.

[9] Y. Song, T.W. Noh, S.I. Lee, J.R. Gaines, Experimental study of the three-dimensional ac conductivity and dielectric constant of a conductor–insulator composite near the percolation thres, Phys. Rev. B 33 (2) (1986) 904–908.

[10] J.W. Hu, M.W. Li, M.Q. Zhang, D.S. Xiao, G.S. Cheng, M.Z. Rong, Preparation of binary conductive polymer composites with very low percolation threshold by latex blending, Macromol. Rapid Commun. 24 (15) (2003) 889–893.

[11] Z.M. Dang, Y.H. Zhang, S.C. Tjong, Dependence of dielectric behavior on the physical property of fillers in the polymer–matrix composites, Synth. Met. 146 (2004) 79–84.

[12] Z.M. Dang, Y.H. Lin, C.W. Nan, Novel ferroelectric polymer composites with high dielectric constants, Adv. Mater. 15 (19) (2003) 1625–1629.

[13] Z.M. Dang, L. Wang, H.Y. Wang, C.W. Nan, D. Xie, Y. Yin, S.C. Tjong, Rescaled temperature dependence of dielectric behavior of ferroelectric polymer composites, Appl. Phys. Lett. 86 (2005) 172905–172907.

[14] C. Huang, J. Su, Q.M. Zhang, High-dielectric-constant all-organic/polymeric composite actuator materials, Mater. Res. Soc. Symp. Proc. 785 (2004) 73–78.

[15] C. Huang, Q.M. Zhang, J. Su, High-dielectric-constant all-polymer percolative composites, Appl. Phys. Lett. 82 (20) (2003) 3502–3504.

[16] C.P. Chwang, C.D. Liu, S.W. Huang, D.Y. Chao, S.N. Lee, Synthesis and characterization of high dielectric constant polyaniline/polyurethane blends, Synth. Met. 142 (2004) 275–281.

[17] C. Pecharromán, J.S. Moya, Experimental evidence of a giant capacitance in insulator–conductor composites at the percolation threshold, Adv. Mater. 12 (4) (2000) 294–297.

[18] W.J. Bae, K.H. Kim, W.H. Jo, Exfoliated nanocomposite from polyaniline graft copolymer/clay, Macromolecules 37 (2004) 9850–9854.

[19] W.M.A.T. Bandara, D.M.M. Krishantha, J.S.H.Q. Perera, R.M.G. Rajapakse, D.T.B. Tennakoon, Preparation, characterization and conducting properties of nanocomposites of successively intercalated polyaniline (pani) in montmorillonite (MMT), J. Compos. Mater. 39 (2005) 759–775.

[20] P. Aranda, M. Darder, R. Fernández-Saavedra, M. López-Blanco, E. Ruiz-Hitzky, Relevance of polymer – and biopolymer – clay nanocomposites in electrochemical and electroanalytical applications, Thin Solid Films 495 (1-2) (2006) 104–112.

[21] J.H. Sung, H.J. Choi, Effect of pH on Physical characteristics of conducting poly(*O*-ethoxyaniline) nanocomposites, J. Macromol. Sci. B: Phys. 44 (3) (2005) 365–375.

[22] A. Dey, S. De, A. De, S.K. De, Characterization and dielectric properties of polyaniline–TiO_2 nanocomposites, Nanotechnology 15 (9) (2004) 1277–1283.

[23] C. Huang, Q.M. Zhang, Fully functionalized high-dielectric-constant nanophase polymers with high electromechanical response, Adv. Mater. 17 (9) (2005) 1153–1158.

[24] J.C. Xu, W.M. Liu, H.L. Li, Titanium dioxide doped polyaniline, Mater. Sci. Eng. C 25 (2005) 444–447.

[25] S.J. Su, N. Kuramoto, Processable polyaniline–titanium dioxide nanocomposites: effect of titanium dioxide on the conductivity, Synth. Met. 114 (2) (2000) 147–153.

[26] F.Y. Chuang, S.M. Yang, Titanium oxide and polyaniline core-shell nanocomposites, Synth. Met. 152 (1–3) (2005) 361–364.

[27] S.P. Armes, S. Gottesfeld, J.G. Beery, F. Garzon, S.F. Agnew, Conducting polymer–colloidal silica composites, Polymer 32 (13) (1991) 2325–2330.